Nanoscale

Cite this: *Nanoscale*, 2011, **3**, 3089

www.rsc.org/nanoscale

COMMUNICATION

Direct growth of graphene pad on exfoliated hexagonal boron nitride surface†

Minhyeok Son, Hyunseob Lim, Misun Hong and Hee Cheul Choi*

Received 17th May 2011, Accepted 18th June 2011
DOI: 10.1039/c1nr10504c

A direct and metal layer-free growth of flat graphene pads on exfoliated hexagonal boron nitride substrate (h-BN) are demonstrated by atmospheric chemical vapour deposition (CVD) process. Round shape with high flatness graphene pads are grown in high yield (~95%) with a pad thickness of ~0.5 nm and homogenous diameter.

Among many extraordinary properties of graphene emerging from its unique geometry of an atomic thick layer, peculiar electronic features including extremely high carrier mobility have attracted great interest for the developments of high performance electronic devices.[1,2] Recent intensive experimental and theoretical studies have revealed that there are two types of scattering factors responsible for the lowering of carrier mobility: intrinsic scatters such as natural phonon scatter in graphene,[3] and non-intrinsic scattering factors such as microscopic ripples (or geometrical flatness) and charged impurities either on graphene itself or from the interaction with dielectric substrate in cases where they are fabricated into field effect transistor.[4,5] There have been many efforts to synthesize graphenes with such non-intrinsic scatters eliminated, and recently a substantially increased carrier mobility (60 000 $cm^2 V^{-1} s^{-1}$) has been demonstrated by replacing the dielectric substrate with an atomically flat hexagonal boron nitride (h-BN) substrate,[6] while a record high carrier mobility has been measured from a suspended graphene device (200 000 $cm^2 V^{-1} s^{-1}$).[7] From a practical point of view, suspended graphene device is mechanically unstable and difficult to fabricate since it requires complicated processes including transferring and positioning of graphene. The process for the preparation of graphene device on h-BN in ref. 6 also requires quite a complicated process due to the intrinsic difficulty of double exfoliation of graphene and h-BN. Therefore, a new strategy for the direct preparation of graphene on h-BN is in high demand.

Graphene growth by chemical vapor deposition (CVD) on catalyst metal film is advantageous over other synthetic methods, especially for large area graphene formation and positioning of graphene at specific locations.[8] However, the metal catalyst-based CVD process holds several problems especially related with catalyst removal and transfer. The synthesis of graphene on non-metal substrates by CVD is currently one of the hot subjects in graphene society, and several groups have reported the formation of few layer graphenes on dielectric substrates. Rümmeli *et al.* have shown that few layer graphenes grow on MgO nanocrystal powders,[9] and Wei *et al.* have found that multilayer graphene nanoribbons can be formed by using ZnS nanoribbon templates.[10] The potential of direct growth of graphene on h-BN has been first realized by Oshima *et al.* in 2000 when they investigated the effect of adlayer on the electrical property of a single h-BN layer epitaxially grown on Ni(111) surface.[11] A similar attempt on h-BN which is pre-grown on Ru(0001) has been recently demonstrated by Bjelkevig *et al.*[12] A direct CVD growth attempted on powder h-BN flakes has been also reported by Ding *et al.*[13] Although the growth of graphene on non-metal substrate becomes assured from the above results, a direct growth of high quality graphene, especially single layer graphene as a major product, on a flat exfoliated h-BN has not yet been demonstrated, so the detail growth process is not available either.

Herein we report a catalyst-free direct growth of high yield graphene pads by CVD process on a h-BN substrate. In our case, all the graphene growth has been attempted and monitored directly on individual flat h-BN disks that are pre-exfoliated on a SiO_2/Si substrate. The graphene grows into a highly regular pad shape with high flatness and surface coverage of >95% of h-BN substrate, and the yield of single layer graphene pad exceeds 90% at specific reaction condition. A plausible growth mechanism is also proposed based on the step-by-step growth results obtained from systematic investigation performed at various reaction conditions.

Flat h-BN disks mechanically exfoliated on a SiO_2/Si wafer generally have diameters of 2–10 μm and 100–300 nm thickness as confirmed by optical and atomic force microscopy (AFM) (Fig. S1†). The powder X-ray diffraction (XRD) pattern shows that the exfoliated h-BN disks are well aligned along the (001) direction on the surface of which there is a hexagonal boron and nitrogen array (Fig. S2†). When a SiO_2/Si substrate containing h-BN disks was heated in the CVD system under 50 sccm of H_2 and 50 sccm of CH_4 at 1000 °C for 120 min, highly regular thin graphene pads are observed as shown in Fig. 1a. The diameter distribution of graphene pads is very narrow with an average diameter of about 108 nm (Fig. S3†). As glanced from the homogeneous height color level of the AFM image, most of the graphene pads have similar thickness as a representative height profile shows about 0.5 nm of thickness

Department of Chemistry and Division of Advanced Materials Science, Pohang University of Science and Technology (POSTECH) San 31, Hyoja-Dong, Nam-Gu, Pohang, 790-784, Korea. E-mail: choihc@postech.edu; Fax: +82 54-279-3399; Tel: +82 54-279-2130

† Electronic supplementary information (ESI) available: Experimental details, AFM image and XRD of h-BN disks, size distribution of graphene pads, quantitative analysis of XPS, and AFM images of control experiment. See DOI: 10.1039/c1nr10504c

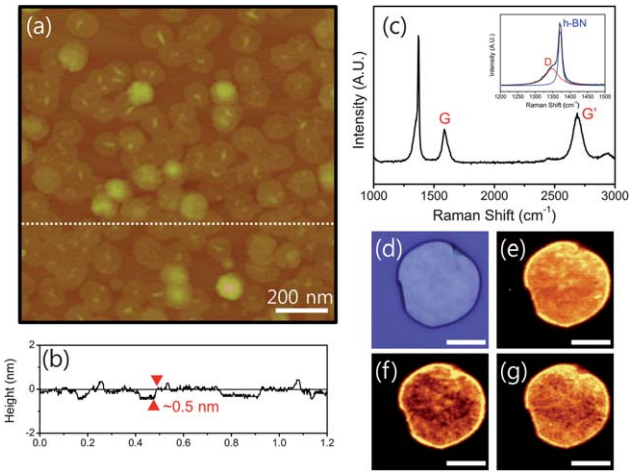

Fig. 1 Graphene pads grown on h-BN by CVD process. (a) Representative AFM image of graphene pads grown at 1000 °C for 120 min under 50 sccm of H_2 and 50 sccm of CH_4. (b) Height profile along the white dotted line indicated in (a). (c) Raman spectrum obtained from (a) showing typical Raman peaks of graphene, D, G, and G′. Inset shows deconvoluted graphene D peak and h-BN peak (E_{2g} mode). (d) Optical image of original h-BN exfoliated on SiO_2/Si substrate. (e–g) Raman images of D (graphene pad) + E_{2g} (h-BN), G, and G′ peaks mapped after growth, respectively. The scale bars in (d–f) are 4 μm.

(Fig. 1b). A statistical AFM data analysis indicates that more than 85% of graphene pads are within this range, and we believe that the graphene pads with such thickness level are single layers.

We have performed Raman spectroscopy that provides information not only about the general quality of graphene by the prominent G and D peaks originated from doubly degenerated zone center E_{2g} mode and defects, respectively, but also about the number of graphene layers and the degree of interaction of graphene with substrate by the G′ peak that connects the phonon wave vector to electronic structure of graphene. In the case of single layer exfoliated graphene on SiO_2/Si, a single G′ peak with G/G′ peak intensity ratio <1 appears, while bilayer graphene shows four G′ peaks since inter-graphene layer coupling splits the peak into four specific components. Our results show that G/G′ peak intensity ratio is <1 and the G′ peak appears at 2689 cm^{-1} which is fitted well with a single Lorentzian with ~70 cm^{-1} of full width at half maximum (FWHM) (Fig. 1c). In some cases of graphene grown on metal substrates, such as Ni,[8a] Cu,[8c] and Ru,[14] bilayer graphene also shows a single G′ peak due to the much diminished inter-graphene layer interaction to the first layer (compared with cleaved one) which has a strong interaction (π–d) with d-electrons of transition metal substrates underneath the graphene. For this reason, the bilayer graphene grown on Ru (0001) shows a single G′ peak while the single layer graphene on Ru (0001) does not even show any Raman signature.[14] However, because there is no strong π–d interaction between the graphene to h-BN, the single G′ peak from graphene pad indicates that most graphene pads are single layers. The FWHM of G′ is quite broad due to relatively large area portion of edge to basal plane in graphene pad,[9b,15] which also results in the broadening of G peak (40 cm^{-1}) compared to exfoliated graphene on SiO_2/Si (15 cm^{-1}).[16] It should be noted that the micro-Raman beam size is ~500 nm, so the exposed sample region contains 10–15 graphene pads including edge boundaries. Also, several thicker layer graphene pads as identified by the brighter height color in AFM image could be included.

The position of G peak also supports the weak interaction of graphene pad to h-BN. The G peak can be shifted by chemical doping including the one induced by charge interaction between graphene and the substrate. The G peak from graphene pad on h-BN appears at 1585 cm^{-1} (Fig. 1c), which is slightly higher than the G peak from exfoliated graphene on SiO_2/Si (1580 cm^{-1}),[17] but lower than the CVD grown ones on Cu (1590 cm^{-1})[8c] and Ru (1599 cm^{-1}).[14] G peak shift can also be induced by strain as demonstrated by graphenes on SiC (1597 cm^{-1}).[18] Based on the G peak position of our case, the strain induced by h-BN seems to be small. We believe that the structural similarity between h-BN (a = 2.504 Å)[19] and graphene (a = 2.468 Å)[20] is responsible for the small strain.

The D peak of graphene pad (1349 cm^{-1}) generally representing the presence of defect disorder is overlapped with an E_{2g} in-plane vibration mode peak of h-BN (1371 cm^{-1}).[21] As shown in Fig. 1c inset, deconvoluted spectra depict the presence of D peak in graphene pads. It is difficult to claim the crystallinity of graphene pad at this stage because the origins of D peak, such as non-graphitized amorphous carbon on h-BN, the edge component of graphene pads, and ripples present in the center of graphene pads, are difficult to be precisely defined due to spectral resolution limit. Meanwhile, the Raman images of h-BN mapped with D, G, and G′ peaks (Fig. 1e–g, respectively) signify that graphene pads grow specifically on h-BN disks but not on SiO_2/Si.

To determine the amount of oxygen, the main element in defect chemical moieties, spatially resolved X-ray photoelectron spectroscopy (SR-XPS) was performed. As shown in the survey spectrum (Fig. 2a) C 1s and O 1s are observed besides B 1s, N 1s, and Si 2p that are originated from the substrates. The high resolution C 1s spectrum in Fig. 2b is deconvoluted into three Lorentzian peaks. The peak corresponding to graphitic carbon (noted as G) appears at 284.6 eV, while the oxygenated carbons (noted as O) are shown at 285.3 eV and 286.2 eV which correspond to the carbons in C–O and C=O bonds, respectively. The O 1s spectrum also shows two oxygen components corresponding to C–O and C=O (Fig. 2c). Through the analysis of C 1s and O 1s spectra, the weight percentage of oxygen is calculated to be only 4%, which shows that the graphene quality is comparable with the graphene grown on metal substrates (see the ESI† for the detail quantitative analysis).[22]

Since one of the inspirations for the direct growth of graphene on h-BN is the high flatness of resulting graphene, we examined the roughness of graphene grown on h-BN. Three-dimensional AFM topographic data shown in Fig. 3a and b visualize a clear difference in surface roughness of graphene on h-BN and bare SiO_2/Si substrate, respectively. The histograms of surface roughness shown in Fig. 3c

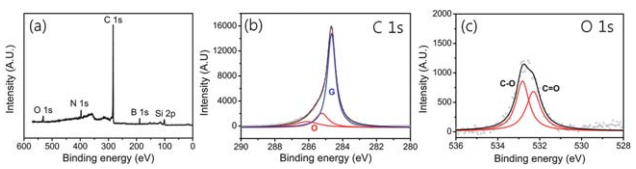

Fig. 2 Spatially resolved X-ray photoelectron spectroscopy (SR-XPS) spectra obtained from graphene pads grown on h-BN. (a) Survey spectrum from 580 to 0 eV showing O 1s, N 1s, C 1s, B 1s, and Si 2p. (b) SR-XPS spectrum around the C 1s, which is deconvoluted into three peaks. O and G represent oxygenated carbons and graphene pad carbons, respectively. (c) SR-XPS spectrum around O 1s region, which shows two oxygen peaks originated from C–O and C=O.

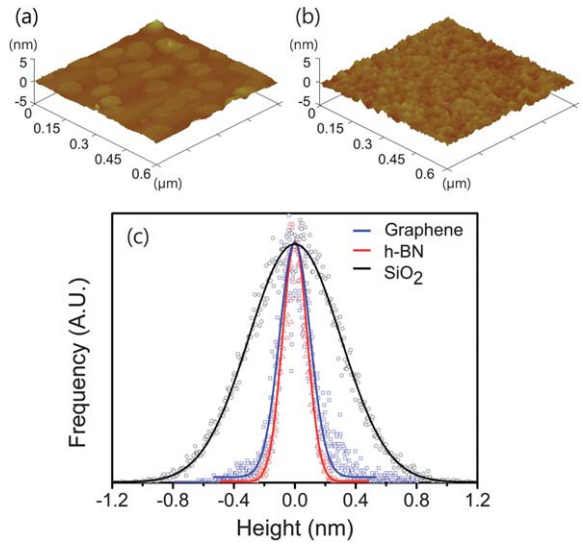

Fig. 3 Topographic AFM images of (a) graphene pads on h-BN and (b) bare SiO_2/Si surface. (c) Histogram of height profiles of graphene pad grown on h-BN (blue), bare h-BN (red), and SiO_2 (black). The solid lines are results of fitting by Gaussian function.

were obtained from bare SiO_2/Si (black curve), bare h-BN (red curve) and graphene on h-BN (blue curve) substrates. For the surface roughness study, graphene pads grown for 60 min was examined to avoid ripples that become popularly present in the center of graphene pad when grown for 120 min (see below for the formation of ripple). The standard deviations (σ) calculated by fitting the distribution curves with Gaussian function are 100 and 80 pm for graphene pad and h-BN, respectively, which are three times lower than the σ value of SiO_2 (300 pm). This result indicates that CVD grown graphene pads resemble the surface flatness of h-BN substrate, which agrees well with the previous results measured from exfoliated graphene transferred on h-BN.[6]

The growth of graphene pad critically depends on the growth condition, such as reaction temperature, precursor gas amount, and reaction time. We first examined the effects of reaction temperature (900–1000 °C) and precursor gas (CH_4) amount (30–50 sccm). As shown in Fig. S5,† graphene pad can grow at temperatures as low as 900 °C with low population, and the population of graphene pad is directly proportional to the reaction temperature. Besides the population, the size distribution of graphene pad is quite wide when grown at temperatures lower than 1000 °C. Meanwhile, the number of graphene pad decreases as the CH_4 content is reduced while the average pad sizes are similar (Fig. S6†). These results indicate that nucleation for graphene pad is controlled by both reaction temperature and precursor amount. A better understanding of the graphene pad growth process has been obtained from time-dependent growth experiments performed at identical conditions used for Fig. 1a. AFM-measureable features start to appear after 10 min of reaction (Fig. 4a). Thermally defragmented carbon precursors (monomer or clusters) are randomly nucleated on h-BN, resulting in the formation of nucleating particles. Although its population is low, nucleating particles with heights of about 0.9 nm as well as small and thin layers around the particles—presumably not a fully developed graphene yet—are clearly observed from a magnified AFM image in Fig. 4b. At this point, there is no clear evidence for a specific nucleation at step edges, of which lowered surface energy frequently initiate graphene nucleation on metals.[9,14] After 30 min of reaction, individual graphene pads are developed in irregular round shapes through peripheral expansion with an average diameter of 60 nm (Fig. 4c). An interesting feature is that most of the graphene pads have semi-bilayers as confirmed by both AFM topographic image and two-step height profile with 0.5 nm of peak height (Fig. 4d), while the original size-confined nucleating particles are difficult to be found. The semi-bilayer means that the top layer does not fully cover the bottom layer of graphene pad, yet it is much too large and flat to be called as a nucleate particle. At this stage, there are three possible ways for carbon sources to be introduced for the propagation of graphene pad growth: (1) surface segregation of carbon into graphene through carbon/h-BN solid solution state, (2) peripheral growth by direct attachment of carbon sources to the edges of graphene pad through surface diffusion, and (3) peripheral growth by carbon sources fed through the nucleate particle acting as a central gateway of carbon precursor. The surface segregation process is excluded because no temperature drop effect has been observed, which is the signature of the segregation growth as observed from graphenes grown on Ru, Ir, and Ni metal substrates.[23] Although the second process of direct attachment of atomic or cluster carbon sources is somewhat contributable,[24,25] the third process involving the nucleate particle as a carbon source gateway seems to dominate the expansion of graphene pad according to the following further growth results. After reaction for 60 min, the graphene pad grows mostly into single layer graphene with very smooth top surface (0.35 nm of height) and an average diameter of 80 nm (Fig. 4e and f). The yield of single layer graphene pad exceeds 90% at this reaction condition. More importantly, the top layer seems to migrate and merge to the bottom layer as confirmed by complete disappearance of second (top) layer, increase of diameter of graphene pad, and reappearance of nucleating particles.

Such a migration of second layer implies that the layer is not fully developed into crystalline graphene yet, which is supported by high D band and low G′ band Raman intensities for the graphene pads grown at a reaction time shorter than 60 min (Fig. 5). The proposed role of nucleate particle that absorbs and delivers carbon precursors is further evidenced by the formation of ripples that start to emerge beyond 90 min of growth time (Fig. 4g and h). Almost all of single layer graphene pads possess the ripples. In general, the ripples on graphene grown by CVD on either metal or insulator substrate are formed by (1) mechanical relaxation during cooling stage owing to different thermal expansion coefficient of graphene and substrate,[26] and (2) merging of neighboring graphenes.[8c,10] However, neither case explains well the current model because the thermal expansion coefficients of h-BN and graphene are similar,[27] and ripples are always formed at the center of graphene pads. Therefore, the origin of the ripple formation is the continuous accumulation of carbon precursors onto the nucleate particle.

The increase of size of graphene pad nearly stops at 90 min with a saturated diameter of about 110 nm (Fig. S7†). Continuous growth attempts for longer than 120 min basically result in the increases of ripple size and number of layers of graphene pad with increased Raman G/G′ peak intensity ratio (Fig. S8†). The reason for the saturation of graphene pad growth is unclear yet, but it seems related to surface interaction of graphene pad and h-BN. In contrast to the graphene grown on metal substrates that employ graphitization from carbon-metal solid solution phase,[23] graphene growth on insulating

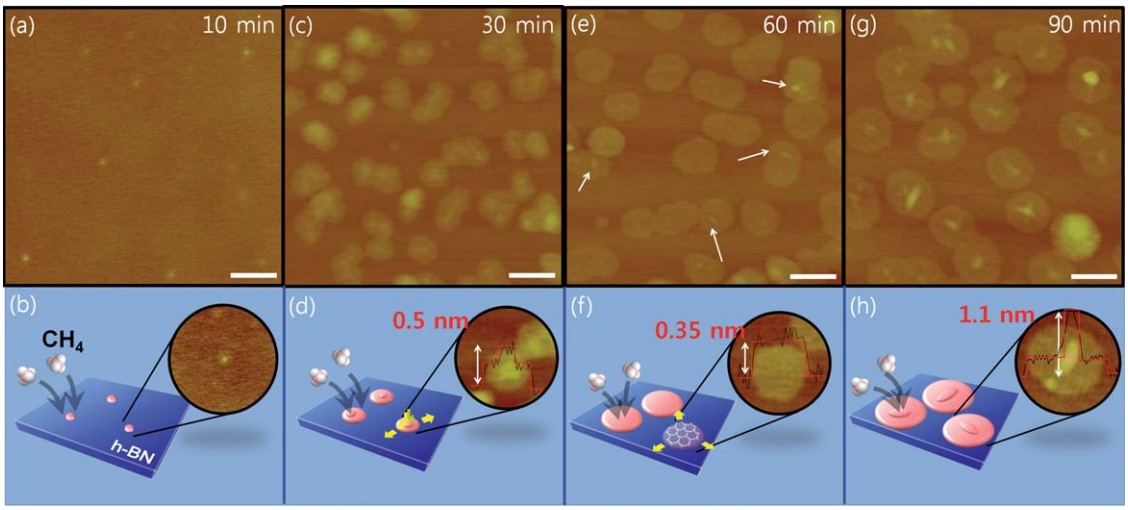

Fig. 4 Time-dependent growth process of graphene pad on h-BN. (a and b) Formation of nucleating particles. (c and d) Formation of semi-bilayer graphene pad as an intermediate. (e and f) Complete formation of single layer graphene pad. (g and h) Emergence of ripple at the center of graphene pad. The scale bars in AFM images are 100 nm.

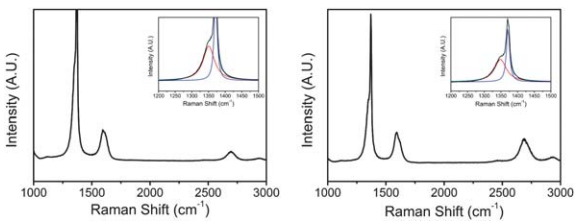

Fig. 5 Raman spectra of graphene pads after (a) 30 min and (b) 60 min. Insets show deconvoluted D peak of graphene and E_{2g} mode h-BN peak. All peaks are normalized by G peak intensities.

substrates deals with direct nucleation and propagation of graphitization on the surface. Although the growth conditions are somewhat different, previous results of graphene grown on a single crystalline sapphire substrate show that a large structural difference for graphene (a = 2.468 Å)[28] to α-Al_2O_3 ((0001), a = 4.762 Å)[29] actually helps to grow graphene even into a film.[30] In the case of h-BN, it seems that the high structural similarity between the graphene pad and h-BN is supposed to induce stronger interaction, especially when the graphene pad becomes larger than a critical size. We are currently investigating more details about the origin of the diameter limit of graphene pad on h-BN.

In summary, we have demonstrated that flat graphene pads can be grown in high population on mechanically exfoliated h-BN surface without metal catalyst by ambient pressure CVD process. The single layer graphene pads have a regular round shape and the size increases up to about 110 nm in diameter, beyond which the number of graphene layers increases. The control studies on reaction temperature and precursor gas amount have revealed that the population and size of graphene pad are directly proportional to those growth parameters. The time-dependent growth study has shown that the growth process involves the formation of nucleate particle and semi-bilayer graphene pad as an intermediate state for the formation of single layer graphene pad through peripheral growth on h-BN surface. Future efforts will be focused on the elucidation of the origin of graphene pad size limit, so that flat single layer graphene could be directly synthesized in larger sizes on h-BN surface. Moreover, with the graphene pad having larger grain size, the general electronic property of such catalyst-free grown graphene on h-BN will be studied by fabricating field effect transistor devices with individual graphene pads as channels.

Acknowledgements

This work was supported by the National Research Foundation of Korea (NRF) grant funded by MEST (2010-0008208, 2010-0029649, 2010-0029711, 2010-00285), KOSEF through EPB center (2010-001779). H.C.C thanks the World Class University (WCU) program (R31-2008-000-10059-0). The SPEM and SR-XPS experiments were performed at 8A1 beamline of the Pohang Accelerator Laboratory (PAL).

References

1 (*a*) A. H. Castro Neto, F. Guinea, N. M. R. Peres, K. S. Novoselov and A. K. Geim, *Rev. Mod. Phys.*, 2009, **81**, 109; (*b*) X. Du, I. Skachko, A. Barker and E. Y. Andrei, *Nat. Nanotechnol.*, 2008, **3**, 491.
2 (*a*) A. K. Geim and K. S. Novoselov, *Nat. Mater.*, 2007, **6**, 183; (*b*) J. – H. Chen, C. Jang, S. Xiao, M. Ishigami and M. S. Fuhrer, *Nat. Nanotechnol.*, 2008, **3**, 206.
3 S. V. Morozov, K. S. Novoselov, M. I. Katsnelson, F. Schedin, D. C. Elias, J. A. Jaszczak and A. K. Geim, *Phys. Rev. Lett.*, 2008, **110**, 016602.
4 F. Schedin, A. K. Geim, S. V. Morozov, E. W. Hill, P. Blake, M. I. Katsnelson and K. S. Novoselov, *Nat. Mater.*, 2007, **6**, 652.
5 E. H. Hwang, S. Adam and S. D. Sarma, *Phys. Rev. Lett.*, 2007, **98**, 186806.
6 C. R. Dean, A. F. Young, I. Meric, C. Lee, L. Wang, S. Sorgenfrei, K. Watanabe, T. Taniguchi, P. Kim, K. L. Shepard and J. Hone, *Nat. Nanotechnol.*, 2010, **5**, 722.
7 (*a*) K. Bolotin, K. J. Sikes, J. Hone, H. L. Stormer and P. Kim, *Phys. Rev. Lett.*, 2008, **101**, 096802; (*b*) S. V. Morozov, K. S. Novoselev, M. I. Katsnelson, F. Schedin, D. C. Elias, J. A. Jaszczak and A. K. Geim, *Phys. Rev. Lett.*, 2008, **100**, 016602.
8 (*a*) A. Reina, X. Jia, J. Ho, D. Nezich, H. Son, V. Bulovic, M. S. Dresselhaus and J. Kong, *Nano Lett.*, 2009, **9**, 30; (*b*) K. S. Kim, Y. Zhao, H. Jang, S. Y. Lee, J. M. Kim, K. S. Kim, J. H. Ahn, J. Choi and B. H. Hong, *Nature*, 2009, **457**, 706; (*c*) X. S. Li, W. W. Cai, J. H. An, S. Kim, J. Nah, D. X. Yang,

R. D. Piner, A. Velamakanni, I. Jung, E. Tutuc, S. K. Banejee, L. Colombo and R. S. Ruoff, *Science*, 2009, **324**, 1312.
9 (*a*) M. H. Rümmeli, C. Kramberger, A. Grüneis, P. Ayala, T. Gemming, B. Büchner and T. Pichler, *Chem. Mater.*, 2007, **19**, 4105; (*b*) M. H. Rümmeli, A. Bachmatiuk, A. Scott, F. Börrnert, J. H. Warner, V. Hoffman, J.-H. Lin, G. Cuniberti and B. Büchner, *ACS Nano*, 2010, **4**, 4206.
10 D. Wei, Y. Liu, H. Zhang, L. Huang, B. Wu, J. Chen and G. Yu, *J. Am. Chem. Soc.*, 2009, **131**, 11147.
11 C. Oshima, A. Itoh, E. Rokuta, T. Tanaka, K. Yamashita and T. Sakurai, *Solid State Commun.*, 2000, **116**, 37.
12 C. Bjelkevig, Z. Mi, J. Xiao, P. A. Dowben, L. Wang, W. Mei and J. A. Kelber, *J. Phys.: Condens. Matter*, 2010, **22**, 302002.
13 X. Ding, G. Ding, X. Xie, F. Huang and M. Jiang, *Carbon*, 2011, **49**, 2522.
14 P. W. Sutter, J.-I. Flege and E. A. Sutter, *Nat. Mater.*, 2008, **7**, 406.
15 (*a*) A. C. Ferrari, *Solid State Commun.*, 2007, **143**, 47; (*b*) A. C. Ferrari and J. Robertson, *Phys. Rev. B: Condens. Matter*, 2000, **61**, 14095.
16 Y. Y. Wang, Z. H. Ni, T. Yu, Z. X. Shen, H. M. Wang, Y. H. Wu, W. Chen and A. T. S. Wee, *J. Phys. Chem. C*, 2008, **112**, 10637.
17 (*a*) A. C. Ferrari, J. C. Meyer, V. Scardaci, C. Casiraghi, M. Lazzeri, F. Mauri, S. Piscanec, D. Jiang, K. S. Novoselov, S. Roth and A. K. Geim, *Phys. Rev. Lett.*, 2006, **97**, 187401; (*b*) H. Lim, J. Lee, H.-J. Shin, H. S. Shin and H. C. Choi, *Langmuir*, 2010, **26**, 12278.
18 Z. H. Ni, W. Chen, X. F. Fan, J. L. Kuo, T. Yu, A. T. S. Wee and Z. X. Shen, *Phys. Rev. B: Condens. Matter Mater. Phys.*, 2008, **77**, 115416.
19 G. Giovannetti, P. Khomyakove, G. Brocks, P. Kelly and J. V. D. Brink, *Phys. Rev. B: Condens. Matter Mater. Phys.*, 2007, **76**, 073103.
20 S. Reich, J. Maultzsch, C. Thomsen and P. Ordejon, *Phys. Rev. B: Condens. Matter*, 2002, **66**, 035412.
21 Y. Shi, C. Hamsen, X. Jia, K. K. Kim, A. Reina, M. Hofmann, A. L. Hsu, K. Zhang, H. Li, Z.-Y. Juang, M. S. Dresselhaus, L.-J. Li and J. Kong, *Nano Lett.*, 2010, **10**, 4134.
22 G. Jo, M. Choe, C.-Y. Cho, J. H. Kim, W. Park, S. Lee, W.-K. Hong, T.-W. Kim, S.-J. Park, B. H. Hong, Y. H. Kahng and T. Lee, *Nanotechnology*, 2010, **21**, 175201.
23 W. J. Arnoult and R. B. McLellan, *Scr. Metall.*, 1972, **6**, 1013–1018.
24 E. Loginova, N. C. Bartelt, P. J. Feibelman and K. F. McCarty, *New J. Phys.*, 2008, **10**, 093026.
25 X. Li, W. Cai, L. Colombo and R. S. Ruoff, *Nano Lett.*, 2009, **9**, 4268.
26 S. J. Chae, F. Güneş, K. K. Kim, E. S. Kim, G. H. Han, S. M. Kim, H.-J. Shin, S.-M. Yoon, J.-Y. Choi, M. H. Park, C. W. Yang, D. Pribat and Y. H. Lee, *Adv. Mater.*, 2009, **21**, 2328.
27 G. L. Belkenkii, E. Yu. Salaev, R. A. Suleimanov, N. A. Abdullaev and V. Ya. Shteinshraiber, *Solid State Commun.*, 1985, **53**, 967.
28 S. Reich, J. Maultzsch, C. Thomsen and P. Ordejon, *Phys. Rev. B: Condens. Matter*, 2002, **66**, 035412.
29 R. W. G. Wyckoff, in *Crystal Structures*, Vol. 2. Wiley, New York, 1964, pp 6.
30 J. Hwang, V. B. Shields, C. I. Thomas, S. Shivaraman, D. Hao, M. Kim, A. R. Wol, G. S. Tompa and M. G. Spencer, *J. Cryst. Growth*, 2010, **312**, 3219.